TECHNISCHE MECHANIK, Band 20, Heft 4, (2000), 339-348
Manuskripteingang: 28. Februar 2000

Postbuckling of a Circular Plate - Comparing Different Solutions

H. Schoop, J. Hornig, T. Wenzel

Axisymmetric problems have been often investigated in the past. Since the problem is one-dimensional, the boundary problem is suitable for analytical investigations and acts as a benchmark for numerical methods. The postbuckling of an elastic circular plate under axisymmetric loading is investigated. An analytical description is given. Solutions by means of the perturbation method and the finite element method (axisymmetric shell element) are introduced. Numerical results are presented.

1 Introduction

The problem considered is the mechanical behaviour of a circular plate undergoing axisymmetric loading. The plate is subjected to a uniform pressure load D in radial direction. The boundary condition of the plate may vary between simply supported and clamped. The displacement in radial direction remains free at the boundary. Thus the plate remains flat if the load does not exceed the buckling load; otherwise it undergoes large deflections. The aim is to develop an analytical expression to estimate the deflection of the midpoint under postbuckling. Only axisymmetric buckling shapes are in consideration.

2 Analytical Solution

2.1 Kinematics

With respect to the axisymmetry the problem can be considered one-dimensional, because the deformation of the plate depends on the radial coordinate only. Hence we go ahead with a small slice of the angle α shown in Figure 1.

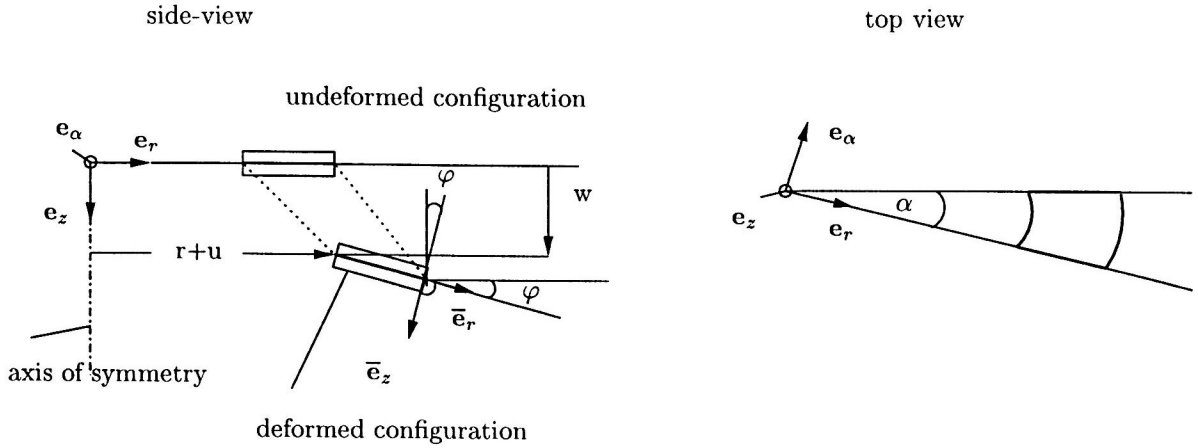

Figure 1: Kinematics of the Plate

The base vectors shown in Figure 1 of the undeformed plate are named $\mathbf{e}_i$ and those in the deformed configuration are denoted by $\bar{\mathbf{e}}_j$.

$$\mathbf{X}(r,z) = r\mathbf{e}_r + z\mathbf{e}_z \tag{1}$$

denotes the position vector before deformation. The deformation consists of displacements in radial (u) and transversal direction (w) and a rotation around the axis $\mathbf{e}_\alpha$. Thus the position vector in the deformed configuration reads

$$\begin{aligned}\mathbf{x}(r,z) &= [r+u(r)]\,\mathbf{e}_r + w(r)\mathbf{e}_z + z\bar{\mathbf{e}}_z \\ &= [r+u(r) - z\,\sin\varphi(r)]\,\mathbf{e}_r + [w(r) + z\,\cos\varphi(r)]\mathbf{e}_z\end{aligned} \tag{2}$$

This kinematic assumption shows that the deformation relies on Kirchhoff's hypothesis. It can be decomposed into stretch and rotation. The rotation tensor $\mathbf{R}$ can easily be found as

$$\begin{aligned}\mathbf{R} &= \mathbf{e}_r \otimes \bar{\mathbf{e}}_r + \mathbf{e}_\alpha \otimes \mathbf{e}_\alpha + \mathbf{e}_z \otimes \bar{\mathbf{e}}_z \\ &= \begin{bmatrix} \cos\varphi & 0 & \sin\varphi \\ 0 & 1 & 0 \\ -\sin\varphi & 0 & \cos\varphi \end{bmatrix} \mathbf{e}_i \otimes \mathbf{e}_j \end{aligned} \tag{3}$$

That means that the slope of the midsurface and the angle of the material normal vector between reference and deformed configuration are the same. For the decomposition of the kinematics the nabla operator is introduced, which allows to calculate the deformation gradient as the derivative of the position vector from equation (2):

$$\mathbf{F} = \nabla \otimes \mathbf{x} \quad \text{with} \quad \nabla = \mathbf{e}_r \frac{\partial}{\partial r} + \frac{1}{r}\mathbf{e}_\alpha \frac{\partial}{\partial \alpha} + \mathbf{e}_z \frac{\partial}{\partial z} \tag{4}$$

Using $(\dots)'$ for the derivative $\frac{\partial}{\partial r}(\dots)$, finally the desired decomposition is gained with equation (3) and equation (4). The right stretch tensor $\mathbf{U}$ follows as

$$\begin{aligned}\mathbf{U} &= \mathbf{F} \cdot \mathbf{R}^t \\ &= \begin{bmatrix} \frac{1+u'}{\cos\varphi} - z\varphi' & 0 & 0 \\ 0 & 1 + \frac{u}{r} - z\frac{\sin\varphi}{r} & 0 \\ 0 & 0 & 1 \end{bmatrix} \mathbf{e}_i \otimes \mathbf{e}_j \end{aligned} \tag{5}$$

Equation (5) neglects the deformation in thickness direction of the plate. The form of $\mathbf{U}$ also expresses the fact that the deformation state is a principal one (with respect to the axisymmetry).

2.2 Strains

The axioms of objectivity and frame indifference require particular variables to be used by formulating constitutive equations if the considered material is hyperelastic. The intention is to relate the Cauchy strains and the Euler stresses in a constitutive law. Thus the left stretch tensor $\mathbf{V}$ is introduced to calculate the stretches expressed in terms of the deformed configuration. As the eigenvalues of $\mathbf{U}$ and $\mathbf{V}$ are the same, the result is easy to achieve: the base vectors have to be replaced. It is found

$$\mathbf{V} = U_{rr}\bar{\mathbf{e}}_r \otimes \bar{\mathbf{e}}_r + U_{\alpha\alpha}\bar{\mathbf{e}}_\alpha \otimes \bar{\mathbf{e}}_\alpha + \bar{\mathbf{e}}_z \otimes \bar{\mathbf{e}}_z \tag{6}$$

From equation (6) the Cauchy strains are derived as

$$\mathbf{E} = \mathbf{V} - \mathbf{1} \tag{7}$$

where $\mathbf{1}$ denotes the second order unit tensor. The strains in the mid-surface of the plate are identified as the terms in z^0

$$\epsilon_{rr} = \frac{1+u'}{\cos\varphi} - 1 \quad \text{and} \quad \epsilon_{\alpha\alpha} = \frac{u}{r} \tag{8}$$

and finally the curvatures - which are the terms in z^1 - turn out as

$$\kappa_{rr} = -\varphi' \quad \text{and} \quad \kappa_{\alpha\alpha} = -\frac{\sin\varphi}{r} \tag{9}$$

Alternatively the state of deformation can be written as

$$\mathbf{E} = (\epsilon_{\beta\gamma} + z\,\kappa_{\beta\gamma})\bar{\mathbf{e}}_\beta \otimes \bar{\mathbf{e}}_\gamma \tag{10}$$

2.3 Equilibrium of Forces and Moments

The conditions of equilibrium are given by equation (11) and equation (12)

$$\bar{\nabla} \cdot (\mathbf{T} + \mathbf{Q}) = \mathbf{0} \tag{11}$$

$$\bar{\nabla} \cdot \mathbf{M} - \mathbf{Q} = \mathbf{0} \tag{12}$$

Here $\mathbf{T}$ represents the membrane stress resultants of the shell's midsurface, $\mathbf{Q}$ denotes the transversal shear force, and $\mathbf{M}$ equals the bending moments. These stress resultants are introduced as Eulerian.

Equation (11) and equation (12) neglect external field loads with respect to the problem in question. To satisfy these conditions the nabla operator $\overline{\nabla}$ for the deformed configuration is calculated. After calculating the metric coefficients and the contravariant components of the base vectors, it is established as

$$\overline{\nabla} = \frac{\cos\varphi}{1+u'}\bar{\mathbf{e}}_r\frac{\partial}{\partial r} + \frac{1}{r+u}\mathbf{e}_\alpha\frac{\partial}{\partial\alpha} \tag{13}$$

Calculating the derivatives according to equation (11) the balance of forces can be expressed as

$$\frac{\cos\varphi}{1+u'}[(r+u)\frac{t_{rr}}{\cos\varphi}]' - t_{\alpha\alpha} = 0 \tag{14}$$

Herein the shear force Q is substituted by the membrane force t_{rr} taking into account that the internal transversal shear force has to vanish in every cross section. The balance of moments is written as

$$\frac{[(r+u)m_{rr}]'}{(1+u')(r+u)} - \frac{m_{\alpha\alpha}}{r+u} + t_{rr}\frac{\tan\varphi}{\cos\varphi} = 0 \tag{15}$$

The two differential equations shall now be transformed in terms of the deformation variables φ and u, which represent the slope of the plate's midsurface and the radial displacement. Therefore a constitutive equation for hyperelastic materials is introduced.

2.4 Constitutive Laws

With the modulus of elasticity E and the Poisson's ratio ν, the plate stiffnesses K_S and K_P are defined as follows (h denotes the thickness of the plate):

$$K_S = \frac{Eh}{1-\nu^2} \quad \text{and} \quad K_P = \frac{Eh^3}{12(1-\nu^2)} \tag{16}$$

With these definitions the equations

$$t_{rr} = K_S\left(\frac{1+u'}{\cos\varphi} - 1 + \nu\frac{u}{r}\right) \quad \text{and} \quad t_{\alpha\alpha} = K_S\left[\frac{u}{r} + \nu\left(\frac{1+u'}{\cos\varphi} - 1\right)\right] \tag{17}$$

are introduced as the internal membrane forces. The bending moments turn out as

$$m_{rr} = -K_P\left(\varphi' + \nu\frac{\sin\varphi}{r}\right) \quad \text{and} \quad m_{\alpha\alpha} = -K_P\left(\frac{\sin\varphi}{r} + \nu\varphi'\right) \tag{18}$$

2.5 Governing Equations

To obtain a system of differential equations for the kinematic variables φ and u the internal stress resultants are now replaced by the constitutive laws introduced in equation (17) and equation (18) . For the slope of the plate φ and for the radial displacement u this yields

$$\frac{\varphi''}{1+u'} + \left(\frac{\varphi'}{r+u} + \frac{\sin\varphi}{r(r+u)}\right)(1+\nu) + \frac{\nu}{1+u'}\left[\frac{\sin\varphi}{r}\right]' - \frac{K_S}{K_P}\frac{\tan\varphi}{\cos\varphi}\left(\frac{1+u'}{\cos\varphi} - 1 + \nu\frac{u}{r}\right) = 0 \tag{19}$$

and

$$\frac{\cos\varphi}{1+u'}\left[\frac{r+u}{\cos\varphi}\left(\frac{1+u'}{\cos\varphi} - 1 + \nu\frac{u}{r}\right)\right]' - \frac{u}{r} + \nu\left(\frac{1+u'}{\cos\varphi} - 1\right) = 0 \tag{20}$$

The system of equation (19) and equation (20) is a strong non-linear system of coupled differential equations. The strategy used to solve this problem is the perturbation method. To perform this technology the trigonometric expressions in equation (19) and equation (20) are being substituted by their power series. Only the second order terms of the power series are taken into account (third order terms respectively) and for the sake of simplicity $\nu = 0$ is choosen. Then equation (19) can be written as

$$\frac{\varphi''}{1+u'} + \frac{\varphi'}{r+u} + \frac{\varphi + \frac{\varphi^3}{6}}{r(r+u)} + \frac{K_S}{K_P}\frac{\varphi + \frac{\varphi^3}{3}}{1-\frac{\varphi^2}{2}}\left(\frac{1+u'}{1-\frac{\varphi^2}{2}} - 1\right) = 0 \tag{21}$$

At this level of investigation the difficulties for an enhanced development are visible. The term $(1-\frac{\varphi^2}{2})^{-1}$ in equation (21) can be substituted by the power series of the function $(1-x)^{\alpha}$ in general. But as a result of the outstanding character of the differential equation (21), the solution is stopped here due to the lack of capable mathematics. The differential equation resembles an equation of the Bessel type. Applying the perturbation method to a differential equation of the Bessel type, an addition theorem for products of Bessel functions is needed. Unfortunately the product of Bessel function leads to an infinite Neumann series as shown by Watson (1966). A simple formula similar to the replacement of $\sin(x)^3$ by $\sin(3x)$ for trigonometric functions cannot be obtained.

2.6 Linearization

To figure out whether the derived equations are reasonable - althought we don't look any further at them due to their strong non-linear character - the linearization is checked. In case of the second order theory equation (19) should yield the differential equation for the buckling of plates, and for the completely uncoupled problem (linear theory) the equation of the plate under strechting should be included. In case of linearization, equation (14) and equation (15) are transformed into

$$t'_{rr} + \frac{t_{rr} - t_{\alpha\alpha}}{r} = 0 \quad \text{and} \tag{22}$$

$$m'_{rr} + \frac{m_{rr} - m_{\alpha\alpha}}{r} - \varphi\, t_{rr} = 0 \tag{23}$$

To switch to the formulation in terms of deformations, the internal stress resultants are being substituted by the constitutive laws. In the sense of the second order theory the product $\varphi\, t_{rr}$ in equation (23) is not small, because t_{rr} remains finite. Thus - if equation (17) and equation (18) are incorporated - equation (19) becomes

$$\varphi'' + \frac{\varphi'}{r} + \left(\frac{D}{K_P} - \frac{1}{r^2}\right)\varphi = 0 \tag{24}$$

Herein D represents the pressure load at the boundary that equals the membrane force t_{rr} in the linear theory. Equation (24) is the classic differential equation for the buckling of a circular plate (Bessel type), as discussed by Timoshenko and Woinowsky-Krieger (1959) or Nádai (1968).
In case of complete uncoupling the product $\varphi\, t_{rr}$ is neglected and the equation of the plate under stretching is generated:

$$u'' + \frac{u'}{r} - \frac{u}{r^2} = 0 \tag{25}$$

From that point of view the linearization check is approved.

3 Solution Based on the von Kármán Equations

The von Kármán equations are

$$K_P \Delta\Delta w = p_z + h\, L(w, F) \tag{26}$$

$$\Delta\Delta F = -\frac{1}{2} E\, L(w, w) \tag{27}$$

where F is the Airy stress function and w the deflection of the plate. The other parameters are used as described in section 2.4. An external load acting in the cross direction is represented by p_z. The operation $L(\Phi, \Psi)$ with Φ and Ψ as scalar value functions is defined by

$$L(\Phi, \Psi) = \Delta\Phi\Delta\Psi - \nabla\nabla\Phi \cdot\cdot \nabla\nabla\Psi \tag{28}$$

These non-linear differential equations describe the behaviour of the plate under moderate rotations - the coupled problem of a plate under bending and stretching. Friedrichs and Stoker (1942) now introduce the two abbreviations

$$p = -\frac{1}{r}\frac{dF}{dr} \quad \text{and} \quad q = -\frac{a}{r}\frac{dw}{dr} \tag{29}$$

and a special operation Γ defined as

$$\Gamma[.] = \frac{1}{a^2 r^3}\frac{d}{dr}\left(r^3\left(\frac{d[.]}{dr}\right)\right) \tag{30}$$

These new variables and the operation Γ perform a useful transformation of equation (26) and equation (27) - as far as the problem is axisymmetric. The quantity p can be interpreted as the radial membrane stress. The value $\frac{r}{R}q$ represents the slope of the deflected plate. The transformations in equation (29) lead to

$$\frac{1}{E}\Gamma[p] = \frac{q^2}{2} \tag{31}$$

$$E\,\Gamma[q] + p\,q = 0 \tag{32}$$

To find a solution firstly the load ratio Λ is introduced:

$$\Lambda = \frac{D}{D_{kr}} \tag{33}$$

where

1. $\Lambda < 1$ means the linear and uncoupled case with the homogeneous stress field $t_{rr} = t_{\alpha\alpha} = -D$. So the plate is just stretched without any curvature.
2. $\Lambda = 1$ denotes the critical condition at the boundary of stabilty.
3. $\Lambda > 1$ is the range of large deflection where this paper focusses on - the postbuckling state.

3.1 Perturbation Method

The proposed solution method is the perturbation method. Friedrichs and Stoker (1942) found this method to manage the problem for ratios of $\Lambda < 2.5$. The functions p and q are expanded in powers of the parameter ϵ that is choosen with

$$\epsilon = \sqrt{\Lambda - 1} \tag{34}$$

The expansion consists of the following form:

$$p = p_0 + \epsilon^2 p_2 + \epsilon^4 p_4 + \epsilon^6 p_6 + \ldots \tag{35}$$

$$q = \epsilon q_1 + \epsilon^3 q_3 + \epsilon^5 q_5 + \ldots \tag{36}$$

Finally this yields a system of linear differential equations for the functions p_k and q_l that will be solved iteratively. The desired solution for the deflection is obtained by integrating the solution $q(r)$ found by the successive solution of the system of equation (35) and equation (36). It yields after intensive calculations

$$w(r) = -\frac{1}{a}\int_0^r q(\bar{r})\,\bar{r}d\bar{r} \tag{37}$$

4 Description of Axisymmetric Shells with a Director Theory

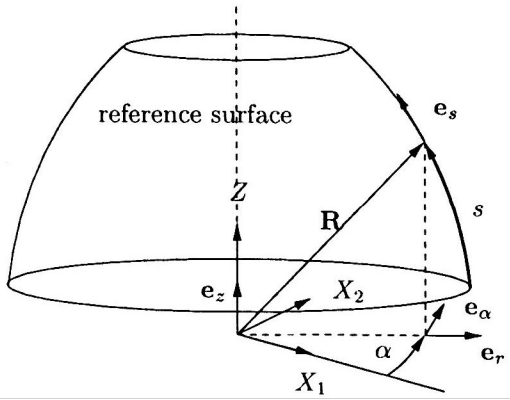

Figure 2: Description of Undeformed Midsurface

Describing the geometry of axisymmetric shells, the following parameters are used: two surface parameters q^λ ($\lambda = 1, 2$) representing a reference surface, usually the shell midsurface, and a thickness parameter η. Vector and tensor components refer to the base vectors $\mathbf{e}_r$, $\mathbf{e}_\alpha$, $\mathbf{e}_s$ or $\mathbf{e}_z$. Note that all of those vectors are unit vectors. The surface parameters q^λ are the circumferential coordinate $q^1 = \alpha$ and the meridional coordinate (arc length) $q^2 = s$ (see Figure 2). Treating large rotations it is distinguished between the reference configuration (undeformed state) and the present configuration (deformed state).

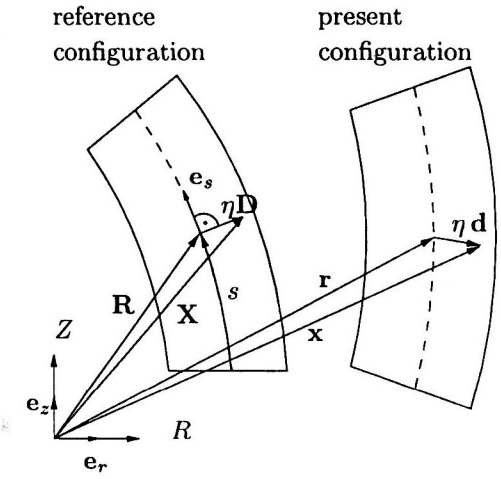

Figure 3: Kinematics of Shell of Revolution

In the reference configuration a material point of the shell $\mathbf{X}(q^\lambda, \eta)$ is characterized by the midsurface postion vector $\mathbf{R}(q^\lambda)$ and a normal vector of that surface $\mathbf{D}(\alpha, s)$:

$$\begin{aligned} \mathbf{X}(q^\lambda, \eta) &= \mathbf{R}(q^\lambda) + \eta\,\mathbf{D}(q^\lambda) \\ &= \mathbf{R}(\alpha, s) + \eta\,\mathbf{D}(\alpha, s) \end{aligned} \tag{38}$$

Here $\mathbf{D} = D_r\mathbf{e_r} + D_z\mathbf{e_z}$ is the unit normal vector of the undeformed midsurface. An analogous representation of a material point in the present configuration $\mathbf{x}(q^\lambda, \eta)$ is given by

$$\begin{aligned} \mathbf{x}(q^\lambda, \eta) &= \mathbf{r}(q^\lambda) + \eta\,\mathbf{d}(q^\lambda) \\ &= \mathbf{r}(\alpha, s) + \eta\,\mathbf{d}(\alpha, s) \end{aligned} \tag{39}$$

The vector $\mathbf{r}(\alpha, s) = r(s)\,\mathbf{e}_r + z(s)\,\mathbf{e}_z$ points to the deformed midsurface. In general the director $\mathbf{d}(\alpha, s) = d_r(s)\,\mathbf{e}_r + d_z(s)\,\mathbf{e}_z$ is not a unit normal vector of the midsurface (see Figure 3). This desciption of shell geometry leans on Naghdi (1972) and Schoop (1987).

4.1 Strains

Describing the state of deformation, contrary to section 2.2 Green's strain tensor $\mathbf{E}^{Green}$ is used. Green's strain tensor is obtained by $\mathbf{E}^{Green} = \frac{1}{2}\left(\mathbf{F}\cdot\mathbf{F}^T - \mathbf{1}\right)$ with $\mathbf{F} = \nabla \circ \mathbf{x}$. The nabla operator refers to the undeformed shell geometry. It is expressed by the approximation

$$\nabla = \frac{1}{R}\mathbf{e}_\alpha\frac{\partial}{\partial\alpha} + \mathbf{e}_s\frac{\partial}{\partial s} + \mathbf{D}\frac{\partial}{\partial\eta} \tag{40}$$

Using the nabla operator and the shell kinematics introduced above, the state of deformation is described as follows. $\mathbf{E}^{Green}$ splits into a part arising from deformation of the midsurface $\varepsilon_{\lambda\mu}$ and into an other part arising from the change of curvature of the midsurface $\kappa_{\lambda\mu}$, depending linearly on η (λ and $\mu = 1, 2$). Furthermore the introduced shell kinematics is suitable for a description of the change of shell thickness and shear deformation. The related strains ε_{33} and $\varepsilon_{\alpha 3}$ are assumed constant over the thickness. The components of $\mathbf{E}^{Green}$ refer to the ($\mathbf{e}_s$, $\mathbf{e}_\alpha$, $\mathbf{D}$)-base. Index 3 relates to the base vector $\mathbf{D}$. Terms containing η^2 are neglected.

4.2 Stress and Moment Resultants

The stress resultants t_{ss}, $t_{\alpha\alpha}$, Q_s and t_3 are obtained by integrating the second Piola-Kirchhoff stresses over the shell thickness of the undeformed state h. For convenience terms containing the curvatures of the reference geometry are neglected. The same remains valid for the moment resultants $m_{\alpha\alpha}$ and m_{ss}. With respect to the axisymmetry of geometry and loading, the stress resultants $m_{s\alpha}$, $m_{\alpha s}$,$t_{s\alpha}$, $t_{\alpha s}$ and Q_α have to equal zero.

4.3 Constitutive Equations

The introduced stress and moment resultants depend on strains and changes of curvature in the following way:

$$\begin{aligned} t_{ss} &= K_S\left(\varepsilon_{ss} + \nu\varepsilon_{\alpha\alpha}\right) & m_{ss} &= K_P\left(\kappa_{ss} + \nu\kappa_{\alpha\alpha}\right) & Q_s &= \frac{Eh}{1+\nu}\varepsilon_{3s} \\ t_{\alpha\alpha} &= K_S\left(\varepsilon_{\alpha\alpha} + \nu\varepsilon_{ss}\right) & m_{\alpha\alpha} &= K_P\left(\kappa_{\alpha\alpha} + \nu\kappa_{ss}\right) & t_3 &= Eh\varepsilon_{33} \end{aligned} \tag{41}$$

The stiffnesses K_S and K_P are introduced in section 2.4. Note that Love's approximation has been applied. Hence we neglect coupling of $\kappa_{\lambda\mu}$, $\varepsilon_{\lambda\mu}$ with $t_{\lambda\mu}$, $m_{\lambda\mu}$, respectively. The constitutive relation regarding t_3 is treated as in case of a uniform state of stress.

5 Numerical Solution with ROSY

The finite element method is used to solve the axisymmetric problem. Therefore the element ROSY developed for a shell of revolution is used. Starting from the principle of virtual work $\delta A^i - \delta A^a = 0$, performing a discretization of the shell structure and applying some standard techniques, a set of equations representing the conditions of equilibrium is established

$$\mathbf{f}^i - \mathbf{f}^a = \mathbf{0} \tag{42}$$

δA^a, δA^i are the virtual work of external loads and virtual internal energy, while $\mathbf{f}^a$, $\mathbf{f}^i$ are the vectors of external and internal loads respectively. The following will focus on internal loads.
Using the constitutive equations introduced in section 4.3 and neglecting the shear strains, the virtual internal energy reads

$$\begin{aligned}\delta A^i &= \int_A \frac{Eh}{1-\nu^2} \Big\{ (\varepsilon_{\alpha\alpha} + \nu\varepsilon_{ss})\,\delta\varepsilon_{\alpha\alpha} + (\nu\varepsilon_{\alpha\alpha} + \varepsilon_{ss})\,\delta\varepsilon_{ss} + (1-\nu^2)\,\varepsilon_{33}\,\delta\varepsilon_{33} + \\ &+ \frac{h^2}{12}(\kappa_{\alpha\alpha} + \nu\kappa_{ss})\,\delta\kappa_{\alpha\alpha} + \frac{h^2}{12}(\nu\kappa_{\alpha\alpha} + \kappa_{ss})\,\delta\kappa_{ss} \Big\}\, dA \end{aligned} \tag{43}$$

The integration has to be carried out over the area of the undeformed midsurface A. Applying the principle of virtual work, the degrees of freedom (the components of the vectors $\mathbf{r}$ and $\mathbf{d}$ in discrete points) have to be varied. Therefore it is necessary to describe strains and changes of curvature in terms of these degrees of freedom.

5.1 Discretization

The axisymmetric shell structure is approximated by ring elements as shown in Figure 4. To obtain this the meridian is divided into a number of line elements, where a is the length of a line element in the reference configuration. The present and the reference configuration are represented by means of the discrete degrees of freedom r_n, z_n, d_{rn}, d_{zn} and discrete values R_n, Z_n, D_{rn}, D_{zn} respectively. Index $n = 1, 2$ is the local node number.

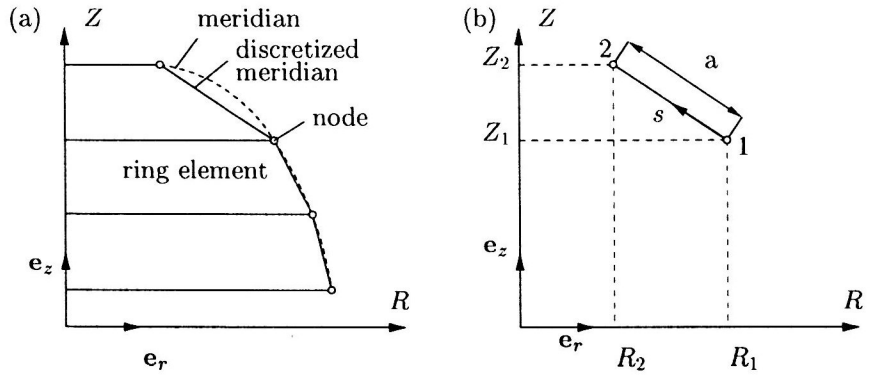

Figure 4: (a) Discretized Shell Structure (b) Local Meridional Coordinate and Local Node Numbering

5.2 Interpolation of Strains

Different methods are applied to express strains and changes of curvature by eight degrees of freedom per element. Linear shape functions

$$L_2 = \frac{s}{a} \qquad L_1 = 1 - L_2 = 1 - \frac{s}{a} \tag{44}$$

will be applied occasionally. $(\ldots)'$ denotes - contrary to its usage in section 2.1 - the derivative $\frac{\partial}{\partial s}(\ldots)$

Strains ε_{ss} and $\varepsilon_{\alpha\alpha}$ are expressed analytically by $\varepsilon_{ss} = \frac{1}{2}\left(r'^2 + z'^2 - 1\right)$ and $\varepsilon_{\alpha\alpha} = \frac{1}{2}\left(\frac{r^2}{R^2} - 1\right)$.
Both, reference and present configuration are interpolated linearly between two nodes:

$$\begin{aligned} R &= L_1 R_1 + L_2 R_2 & Z &= L_1 Z_1 + L_2 Z_2 \\ r &= L_1 r_1 + L_2 r_2 & z &= L_1 z_1 + L_2 z_2 \end{aligned} \tag{45}$$

Hence we get

$$\varepsilon_{ss} = \frac{1}{2}\left(\frac{(r_2 - r_1)^2 + (z_2 - z_1)^2}{a^2} - 1\right) \tag{46}$$

and

$$\varepsilon_{\alpha\alpha} = \frac{1}{2}\left(\frac{(L_1 r_1 + L_2 r_2)^2}{(L_1 R_1 + L_2 R_2)^2} - 1\right) \tag{47}$$

Thickness strain ε_{33} in a node n reads $\varepsilon_{33\,n} = \frac{1}{2}(d_{rn}d_{rn} + d_{zn}d_{zn} - 1)$. Linear interpolation of the strain ε_{33} between the nodes of an element yields

$$\begin{aligned} \varepsilon_{33} &= L_1 \varepsilon_{33\,1} + L_2 \varepsilon_{33\,2} \\ &= \frac{1}{2}\left(L_1 (d_{r1}d_{r1} + d_{z1}d_{z1}) + L_2 (d_{r2}d_{r2} + d_{z2}d_{z2}) - 1\right) \end{aligned} \tag{48}$$

Change of curvature $\kappa_{\alpha\alpha}$ The shell element presented here makes use of a mean bending strain

$$\kappa_{\alpha\alpha m} = \frac{r_m}{R_m^2}\left(d_{rm} - D_{rm}\frac{r_m}{R_m}\right) \tag{49}$$

The mean values D_{rm}, d_{rm} of the vector components D_r and d_r are approximated by radial components of the vectors **N** and **n** (see Figure 5) .

$$D_{rm} \approx \frac{Z_2 - Z_1}{a} \quad d_{rm} \approx \frac{z_2 - z_1}{a} \qquad R_m = \frac{1}{2}(R_2 + R_1) \quad r_m = \frac{1}{2}(r_2 + r_1) \tag{50}$$

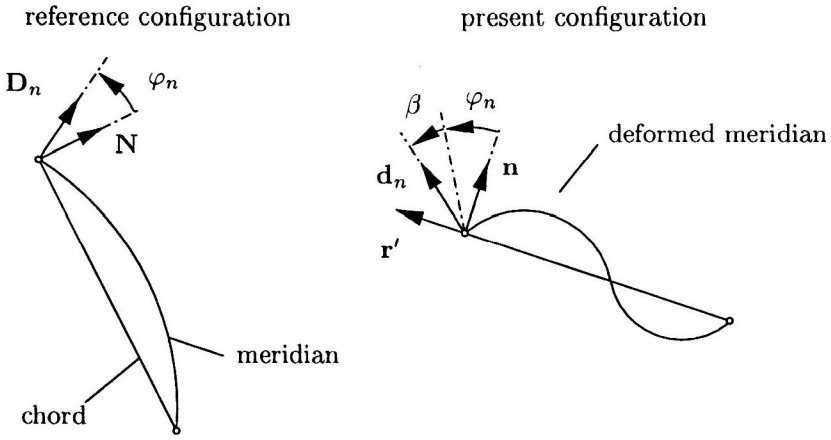

Figure 5: Kinematics of the Deformed Meridian

Change of curvature κ_{ss} Neglecting shear strains and following the notion of DKT (discrete Kirchhoff theory) as discussed by Bathe (1990), κ_{ss} is represented by the change of slope of the deformed meridian $\kappa_{ss} = \frac{\partial\beta}{\partial s}$, still being aware that the material meridional coordinate s refers to the undeformed state. Assuming the nodal values β_1, β_2 as known, the slope in the interior of the element can be interpolated quadratically:

$$\beta(s) = \beta_1 L_1 (L_1 - 2L_2) + \beta_2 L_2 (L_2 - 2L_1) \tag{51}$$

This is equivalent to a cubic interpolated meridian around the chord. The determination of the slope β_n at a node n will be shown next.
Because equation (45) $\mathbf{r}'$ is the chord vector of the element as shown in Figure 5. Bearing in mind that $\beta_n + \varphi_n$ is the complementary angle to that specific angle included by $\mathbf{d}_n$ and $\mathbf{r}'$, the relation

$$\mathbf{d}_n \cdot \mathbf{r}' = (1 + \varepsilon_{33})(1 + \varepsilon_{ss}) \sin(\beta_n + \varphi_n) \tag{52}$$

is achieved. Neglecting ε_{33}, ε_{ss} and assuming small angles φ_n, β_n one can express the slope β_n in a quite simple manner

$$\beta_n = \mathbf{d}_n \cdot \mathbf{r}' - \varphi_n \tag{53}$$

Now the differentiation of equation (51) yields

$$\kappa_{ss} = -\frac{2\beta_1}{a}(2L_1 - L_2) + \frac{2\beta_2}{a}(2L_2 - L_1) \tag{54}$$

5.3 Element Stiffness Matrix

To assemble and to solve the system of non-linear equations (42) a numerical two point integration and Newton's method are applied. It is necessary to determine the global stiffness matrix

$$\mathbf{K} = \frac{\partial(\mathbf{f}^i - \mathbf{f}^a)}{\partial \mathbf{a}} \tag{55}$$

during the iteration process. The vector of the global degrees of freedom **a** contains the nodal values of the components of **r** and **d**. With the prescribed representation of kinematic quantities the formulation of the stiffness matrix is straightforward.

6 Numerical Example

To test the reliability of ROSY a simply supported circular plate with the following data is considered:

$$a = 100[mm] \tag{56}$$
$$h = 1[mm] \tag{57}$$
$$E = 70[\frac{kN}{mm^2}] \tag{58}$$
$$\nu = 0.318 \tag{59}$$

The Poisson's ratio is typical for alloys consisting of aluminium. For easy comparison the simply supported plate was choosen. A further reference for the boundary problem of the clamped plate is discussed by Bodner (1954) using the same method of solution like Friedrichs and Stoker (1942). The numerical solution for the clamped plate is easily achieved by blocking the degrees of freedom for the directors at the boundary $r = a$.
Relating the numerical solution to the solution of Friedrichs and Stoker (1942), the slope φ at the boundary and the deflection w of the plate midpoint were calculated. The values are normalized according to the reference values for the sake of comparability. The solid line in Figure 6 shows the deflection w_0 of the plate midpoint over the load ratio Λ. The dashed line denotes the slope φ_a at the boundary of the plate. The values calculated analytically by the perturbation method are marked with squares and rhombs, respectively.

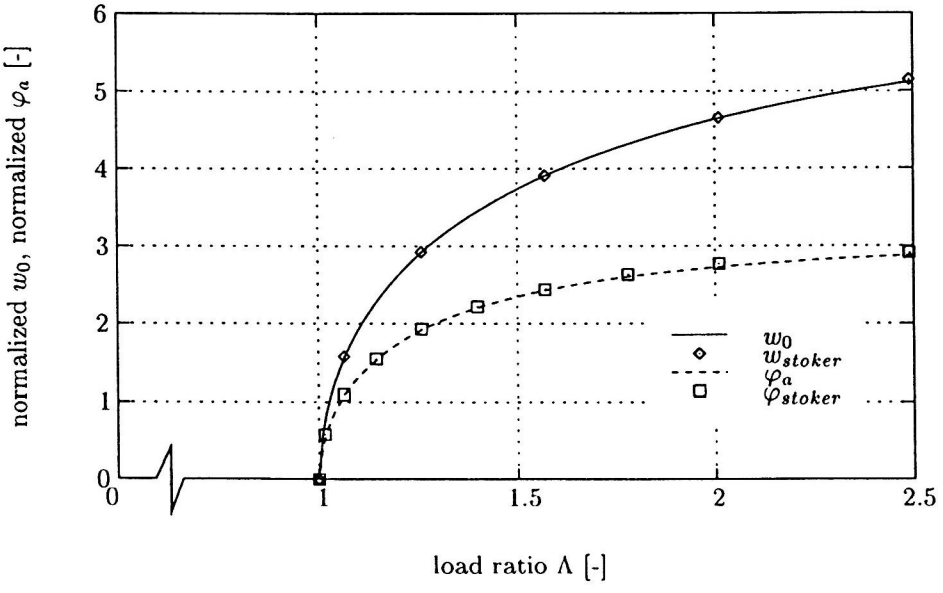

Figure 6: Perturbation Method and FEM in Comparison

w_0 and φ_a both remain equal zero while Λ does not exceed the critical thrust, because no buckling occurs in that load range. At the critical load the non-linear part of the load/deformation-curve begins. The

coincidence of the numerical values calculated by ROSY and the values estimated by the power series method is quite good.
Studying the convergence a number of ten elements per radius was found out to perform well. The analytical buckling load yields $D_{kr} = \lambda^2 \frac{K_P}{a^2}$ where λ is the eigenvalue of the equation

$$\lambda J_0(\lambda) = (1 - \nu) J_1(\lambda) \tag{60}$$

$J_0(\lambda), J_1(\lambda)$ denote the Bessel functions of order zero and one, respectively. The critical load calculated by ROSY and the analytical value differ less than 0.1% if more than five elements are used.

7 Summary

The postbuckling of an elastic circular plate under axisymmetric loading was investigated. The analytical description by means of a third order theory did not convince due to the strong non-linear character of the governing equations. Otherwise the pertubation method introduced by Friedrichs and Stoker (1942) confirms the FEM results achieved by ROSY. Hence a rare non-linear analytical solution verifies the applicability of the ROSY-element.

Literature

1. Bathe, K.-J.: Finite-Elemente-Methoden. Springer-Verlag, (1990).
2. Bodner, S. R.: The postbuckling behaviour of a clamped circular plate. Quarterly Journal of Applied Mathematics, 12, (1954), 397-401.
3. Friedrichs, K. O.; Stoker, J. J.: Buckling of a circular plate beyond the critical thrust. Journal of Applied Mechanics, 9, (1942), A7-A14.
4. Nádai, A.: Die elastischen Platten. Springer-Verlag, (1968).
5. Naghdi, P. M.: The Theory of Shells and Plates. In: Handbuch der Physik/Encyclopedia of physics, Bd. VIa/2, (1972).
6. Schoop, H.: Schalentheorie mit 6 kinematischen Freiheitsgraden bei großen Verschiebungen. Z. angew. Math. Mech., 67, 4, (1987), T237-T239.
7. Timoshenko, S. P.; Woinowsky-Krieger, S.: Theory of plates and shells. McGraw Hill, (1959).
8. Watson, G. N.: A treatise on the theory of Bessel Functions. Cambridge University Press, (1966).

Address: Prof. Dr.-Ing. Heinrich Schoop, Dipl.-Ing. Jörg Hornig, Dipl.-Ing. Thomas Wenzel, Institut für Mechanik - Sekr. J 14, TU Berlin, Jebensstr. 1, D-10623 Berlin